Journal of Quantitative Spectroscopy & Radiative Transfer 272 (2021) 107820

Contents lists available at ScienceDirect

Journal of Quantitative Spectroscopy & Radiative Transfer

journal homepage: www.elsevier.com/locate/jqsrt

Compton ionization of atoms as a method of dynamical spectroscopy

O. Chuluunbaatar[a,b], S. Houamer[c], Yu. V. Popov[a,d,*], I.P. Volobuev[d], M. Kircher[e], R. Dörner[e]

[a] Joint Institute of Nuclear Research, Dubna, Moscow Region 141980, Russia
[b] Institute of Mathematics and Digital Technology, Mongolian Academy of Sciences, Ulaanbaatar 13330, Mongolia
[c] Faculty of Science, University Setif-1, 19000, Setif, Algeria
[d] Skobeltsyn Institute of Nuclear Physics, Lomonosov Moscow State University, Moscow 119991, Russia
[e] Institut für Kernphysik, J. W. Goethe Universität, Max-von-Laue-Str. 1, D-60438 Frankfurt, Germany

ARTICLE INFO

Article history:
Received 13 April 2021
Revised 24 June 2021
Accepted 24 June 2021
Available online 25 June 2021

Keywords:
Methods of dynamical spectroscopy
Compton single ionization

ABSTRACT

In a recent paper published in the journal Nature physics [1], a possibility to measure the fully differential cross section of the reaction of single Compton ionization of a helium atom without detecting the scattered photon has been demonstrated. A comparison of the experimental data with the theory based on the Kramers-Heisenberg-Waller model has shown a good applicability of this model to the case of low (of the order of several keV) photon energies. In the present paper, the possibility of using such reactions for studying the momentum distribution of the active electron in the target atoms is discussed in more detail. We also make a comparison of Compton momentum spectroscopy method with widely known electron momentum spectroscopy.

1. Introduction

Recently, an international research team has carried out a kinematically complete experimental measurement of Compton ionization cross sections of free helium atoms at synchrotron Petra III (DESY, Hamburg) with the COLTRIMS detector (COLd Target Recoil Ion Momentum Spectroscopy) and gave an adequate theoretical description of the obtained results. In the experiment, Compton scattering of photons with the energy of 2.1 keV by helium atoms was studied near the ionization threshold, i.e. the reactions, in which the transferred energy was close to the potential of single ionization of the helium atom $I_p = 24.6$ eV. A comparison of the experimental cross sections with the theoretical ones calculated in the Kramers-Heisenberg-Waller approximation (also called A^2 approximation) [2,3] with various initial and final trial wavefunctions of the atom has shown a sensitivity of the fit quality to the choice of the wave functions [1].

A theoretical description of Compton scattering by free electrons was given almost a hundred years ago independently by Compton [4] and Debye [5] based on the concept of the photon as a relativistic particle. However, this description completely disregarded the effects of electron boundness in the atoms. These effects were first considered by DuMond [6], who, shortly after the development of quantum mechanics and the description in its framework of the atomic structure, made the assumption based on the results of his experiments that Compton scattering can be used for exploring the structure of the atoms of the scatterer. He associated the broadening of the energy spectrum observed at a fixed scattering angle with the momentum distribution of the electrons bound in the material of the scatterer and, having considered several trial momentum distributions for various electronic states, found that the structure of the observed spectrum of the radiation scattered by beryllium atoms is well reproduced theoretically using the quantum mechanical description of bound electrons in the atoms.

Since the time of Compton's experiments, the researches in this field have been based on the coincidence method for simultaneous detection of the electron emitted as a result of the ionization and the scattered photon, which was proposed by the German physicists Bothe and Geiger [7] just for studying the Compton effect in 1924. However, the use of the electron-photon coincidence method for precision measurements was impossible because of a number of technical restrictions. The situation changed with the development of a new method of registration of charged scattered particles, called COLTRIMS [8], and there appeared a real opportunity to use Compton scattering to determine the angular and energy spectra of both the scattered photons and the electrons emitted as a result of a single ionization. The COLTRIMS method allows one to simultaneously measure the momenta of the electron and the recoil ion, which makes it possible to carry out measurements by the coincidence method with high accuracy. In particular, using this technique, it became possible to collect the ions and electrons from

* Corresponding author.
E-mail address: popov@srd.sinp.msu.ru (Yu. V. Popov).

https://doi.org/10.1016/j.jqsrt.2021.107820
0022-4073/

almost the total solid angle $\Omega_{tot} = 4\pi$. In this case, the momentum of the scattered photon can be found from the law of momentum conservation, which eliminates the necessity to detect it. Often this is just impossible in experiments with atoms, because the cross sections are extremely small (about a million times smaller than the typical cross sections of photoionization), and it takes a very long time to collect the necessary statistics.

In quantum electrodynamics, the standard theory of Compton ionization is based on two Feynman diagrams of the second order (see, for example, [9]). However, in the case of photons with energies of several (and even several tens of) keV, one can consider the description of this process using the non-relativistic Schrödinger equation [10]. As a result, the matrix element corresponding to these diagrams splits into the sum of two terms. Both these terms are of the second order in the fine structure constant α, but the form of the first term, traditionally denoted A^2, resembles that of the first Born approximation (FBA) in the case of the atom ionization by a charged particle (proton, electron), and the form of the second (integral) term coincides with that of the second Born approximation (SBA). For a sufficiently high photon energy, the main contribution to the amplitude is given by the FBA term, and the second term turns out to be small and can be viewed as a correction [11].

This theoretical model turned out to be fairly simple, which allowed us to consider a number of trial functions of the initial and final states and to compare the results with the experiment, as well as to estimate the possibility of this new method to carry out a precision spectroscopy (angular and energy) of the outer shells of atoms (molecules). At the same time, the experiment distinguished between the sets of the trial functions, which showed the possibility of using Compton ionization along with the well-known spectroscopic methods such as (e, 2e) (electron impact ionization), (p, pe) (proton impact ionization), etc. In the theory of single ionization of a target by a fast projectile particle, two types of reactions are distinguished depending on the value of the momentum transfer Q. Reactions with low momentum (and energy) transfer from a projectile to a target atom make it possible to better distinguish between the models of the final state functions, and their fully differential cross sections (FDCS) are less sensitive to the details of the one-particle wave function of the active electron in the atom, as well as to (ee) - correlations in the target. Such reactions are called binary. On the contrary, in the case of reactions with large momentum (and energy) transfer, the final wave function simplifies greatly, and the FDCS reveals individual details of the momentum distribution of an electron in an atom (molecule). Such reactions are called quasielastic.

Thus, the experimental and theoretical results recently published in [1], showed new possibilities of Compton ionization of atoms as a method of dynamical spectroscopy of the active electron. This became possible due to the precision measurements of very small differential cross-sections using modern techniques. As a result, the attempts of the pioneers to use the Compton effect discovered almost a hundred years ago for the purpose of spectroscopy of quantum objects with the help of their unsophisticated devices, nowadays received a new impetus.

For a sufficiently high photon energy, Compton ionization reactions allow one to vary the momentum transfer over a wide range, which makes it possible to study both types of reactions in one experiment. The theoretical interpretation of the final state of a target is also greatly simplified. Thus, in this paper, we focus on large momentum transfers in the Compton ionization reaction (below we shortly call them CMS – Compton momentum spectroscopy), and make a comparison of such reactions with $(e, 2e)$ reactions in the kinematics of electron momentum spectroscopy (EMS), which now give a valuable information about the wave function of the active electron in the target [12,13].

The atomic units $e = m_e = \hbar = 1,\ c = 137$ are used throughout the paper, unless it is stated otherwise.

1.1. General formulas

As it has been already noted in the Introduction, nowadays the standard theoretical description of Compton scattering at free and bound electron is carried out in the framework of QED. However, the rigorous relativistic approach contains a series of logical difficulties, namely:

1. In QED, the ion is considered not as a particle, but as a source of an external classical Coulomb field. Of course, such a consideration is admissible due to the huge ion mass M_{ion}. However, in the COLTRIMS detector, where the ion is detected and its momentum is measured, it moves and behaves like a particle.
2. It is extremely challenging to construct a trial wave function of an atom with electron correlations.
3. It is also very difficult to find Green's function of an electron in the Coulomb field of the ion.

However, historically the description of the Compton effect was carried out with the help of the time-dependent non-relativistic Schrödinger equation, which is quite adequate even for photon energies of several tens of keV and low electron energies up to a hundred eV. At such energies, the ion remains practically at rest during the reaction and acquires a momentum $\mathbf{K}$. The energy-momentum conservation laws are written in the form:

$$\omega_1 = \omega_2 + I_p + E_e + E_{ion} \tag{1.1}$$

$$\mathbf{k_1} = \mathbf{k_2} + \mathbf{p} + \mathbf{K} \tag{1.2}$$

In Eq. (1), I_p is the single ionization potential of the helium atom, E_e ($\mathbf{p}$) is the energy (momentum) of the emitted electron, E_{ion} ($\mathbf{K}$) is the energy (momentum) of the residual ion, and ω_i ($\mathbf{k_i}$) stands for energy (momentum) of the initial (final) photon. The momentum transfer is $\mathbf{Q} = \mathbf{k_1} - \mathbf{k_2} = \mathbf{p} + \mathbf{K}$.

Let us write down the Schrödinger equation for the helium atom with a vector-potential $\mathbf{A}$ of electromagnetic field:

$$\begin{aligned} i\frac{\partial}{\partial t}\Psi(\mathbf{r_1},\mathbf{r_2},\mathbf{r_n},t) = \Bigg[&\frac{1}{2}\left(-i\nabla_{\mathbf{1}} - \frac{1}{c}\mathbf{A}(\mathbf{r_1},t)\right)^2 \\ &+\frac{1}{2}\left(-i\nabla_{\mathbf{2}} - \frac{1}{c}\mathbf{A}(\mathbf{r_2},t)\right)^2 + \frac{1}{8M}\left(-i\nabla_{\boldsymbol{n}} + \frac{1}{c}\mathbf{A}(\mathbf{r_n},t)\right)^2 \\ &-\frac{2}{|\mathbf{r_n}-\mathbf{r_1}|} - \frac{2}{|\mathbf{r_n}-\mathbf{r_2}|} + \frac{1}{|\mathbf{r_1}-\mathbf{r_2}|}\Bigg]\Psi(\mathbf{r_1},\mathbf{r_2},\mathbf{r_n},t). \end{aligned} \tag{2}$$

In Eq. (2) $M = 1836$ a.u. is the proton mass, $\mathbf{r_n}$ is the coordinate of the nucleus, and $\mathbf{r_{1,2}}$ denote the coordinates of the electrons. Here, we will not use the second quantized operator of electromagnetic field, but rather define the vector potential as follows:

$$\frac{1}{c}\mathbf{A}(\mathbf{r},t) = \sqrt{\frac{2\pi}{\omega_1}}\ \mathbf{e_1}\ e^{i(\mathbf{k_1}\mathbf{r}-\omega_1 t)} + \sqrt{\frac{2\pi}{\omega_2}}\ \mathbf{e_2}\ e^{-i(\mathbf{k_2}\mathbf{r}-\omega_2 t)} + c.c. \tag{3}$$

In this formula $\mathbf{e_1}$ ($\mathbf{e_2}$) denotes the vector of the linear polarization of the initial (final) photon. Such a choice of the vector potential corresponds to the normalization of the photon wave function to one photon per unit volume and allows to describe processes with one absorbed and one emitted photon. We recall that $(\mathbf{k_i}\cdot\mathbf{e_i}) = 0$, so $\mathrm{div}\mathbf{A}(\mathbf{r},t) = 0$, which corresponds to the Coulomb gauge of the field.

The term describing the interaction of an electron with the field can be written down as

$$V_{int} = i\frac{1}{c}(\mathbf{A}(\mathbf{r},t)\cdot\nabla_{\mathbf{r}}) + \frac{1}{2c^2}A^2(\mathbf{r},t) \tag{4.1}$$

$$= i\left(\sqrt{\frac{2\pi}{\omega_1}}e^{i(\mathbf{k_1}\mathbf{r}-\omega_1 t)}(\mathbf{e_1}\cdot\nabla_{\mathbf{r}}) + \sqrt{\frac{2\pi}{\omega_2}}e^{-i(\mathbf{k_2}\mathbf{r}-\omega_2 t)}(\mathbf{e_2}\cdot\nabla_{\mathbf{r}})\right)+$$

$$\left(\frac{\pi}{\omega_1}+\frac{\pi}{\omega_1}\ e^{2i(\mathbf{k_1}\mathbf{r}-\omega_1 t)}+\frac{\pi}{\omega_2}+\frac{\pi}{\omega_2}\ e^{-2i(\mathbf{k_2}\mathbf{r}-\omega_2 t)}\right)+ \tag{4.2}$$

$$\frac{2\pi}{\sqrt{\omega_1\omega_2}}(\mathbf{e_1}\cdot\mathbf{e_2})e^{i[(\mathbf{k_1}-\mathbf{k_2})\mathbf{r}-(\omega_1-\omega_2)t]} + c.c. \tag{4.3}$$

The term in Eq. (4.3) just defines the A^2 approximation in the Compton scattering theory. Two more terms relevant for this process are the terms in Eq. (4.1), which describe the successive absorption and emission of photons by an electron taking into account intermediate Green's function of the atom. These interaction terms will not be considered here, because their contribution is small for a relatively high photon energy, and it was investigated in more detail for the case of the hydrogen atom in our recent paper [11].

Further, calculating the ionization cross section, carrying out standard operations and omitting details, we

1. neglect the interaction of the nucleus with the field, since it is inversely proportional to the mass of the nucleus (which is also valid in the relativistic treatment);
2. integrate the matrix element with respect to the time t and the coordinate of the ion $\mathbf{r_n}$, which, since we have neglected the interaction with the field, describe the uniform motion of the atom and give the corresponding delta functions of energy and momentum conservation;
3. neglect the energy of the residual ion in the law of energy conservation, because $E_{ion} = K^2/8M$, and the ion mass $4M$ is huge;
4. perform further integrations, removing the delta functions.

Consequently, we obtain the FDCS of the single ionization of an atom by Compton scattering

$$FDCS \equiv \frac{d^3\sigma}{dE_e d\Omega_e d\Omega_1} = \frac{\alpha^4}{(2\pi)^3}\ p\left(1-\frac{E_e+I_p}{\omega_1}\right)\frac{1}{2}\sum_{e_1,e_2}|M|^2. \tag{5}$$

The summation in Eq. (5) implies averaging over the initial polarization $\mathbf{e_1}$ and the summation over the final $\mathbf{e_2}$ polarization of the photon. The matrix element has the form

$$M(\mathbf{Q},\mathbf{p}) = (\mathbf{e_1}\cdot\mathbf{e_2}) < \Phi_f^-(\mathbf{p})|\sum_{j=1}^{2} e^{i\mathbf{Q}\mathbf{r_j}}|\Phi_0 > . \tag{6}$$

Since the initial $< \mathbf{r_1},\mathbf{r_2}|\Phi_0 >$ and final $< \Phi_f^-(\mathbf{p})|\mathbf{r_1},\mathbf{r_2} >$ wave functions can be trial and do not need to be the eigenfunctions of the Hamiltonian of the helium atom, they should be orthogonalized in order that the matrix element $M(\mathbf{Q},\mathbf{p}) = 0$ at $\mathbf{Q} = 0$. We choose the standard recipe of orthogonalization and replace

$$\Phi^{-*}(\mathbf{p};\mathbf{r_1},\mathbf{r_2}) \to \Phi^{-*}(\mathbf{p};\mathbf{r_1},\mathbf{r_2}) - \langle\Phi^-(\mathbf{p})|\Phi_0\rangle\Phi_0(\mathbf{r_1},\mathbf{r_2}),$$

as well as take into account the symmetrization by introducing the factor $1/\sqrt{2}$.

In this formula, the symmetric trial function of the initial state of the helium atom $\Phi_0(\mathbf{r_1},\mathbf{r_2})$ may include electron correlations of various degrees, and the simple final function is chosen in its asymptotic form

$$\Phi_f^{-*}(\mathbf{p};\mathbf{r_1},\mathbf{r_2})$$

$$= \frac{1}{\sqrt{2}}[\varphi^{(*-)}(\mathbf{p},\mathbf{r_1};Z)\varphi_0^{He+}(r_2) + \varphi^{(*-)}(\mathbf{p},\mathbf{r_2};Z)\varphi_0^{He+}(r_1)]. \tag{7}$$

with

$$\varphi_0^{He+}(r) = \sqrt{\frac{8}{\pi}}\ e^{-2r},\ \ \varphi^{(*-)}(\mathbf{p},\mathbf{r};Z)$$

$$= e^{-\pi\zeta/2}\Gamma(1+i\zeta)e^{-i\mathbf{p}\cdot\mathbf{r}}\ {}_1F_1[-i\zeta,1;i(pr+\mathbf{p}\cdot\mathbf{r})].$$

The Coulomb function $\varphi^{(*-)}(\mathbf{p},\mathbf{r};Z)$ depends on the effective ion charge $Z = -p\zeta$, that the electron feels when leaving the atom. Asymptotically $Z = 1$, but inside the atom it can also depend on the radius r.

Let us now discuss the matrix element in Eq. (6). It has been derived as the second order term in the A^2 model, but from the point of view of scattering of a charged particle (electron, proton) by an atom, this matrix element has the structure of the plane-wave first Born approximation (PWFBA). The singlet symmetry of all wave functions and that of the transition operator enable us to group the terms in Eq. (7) in such a way that the variable $\mathbf{p}$ in the integrands in Eq. (6) mates to the variable $\mathbf{r_1}$. As a result, we get

$$\frac{1}{2}\sum_{e_1,e_2}|M|^2 = (1+\cos^2\theta)|T_1+T_2-2T_3|^2, \tag{8}$$

where

$$T_1(\mathbf{p},\mathbf{Q}) = \langle\tilde{\Phi}^-(\mathbf{p})|e^{i\mathbf{Q}\cdot\mathbf{r_1}}|\Phi_0\rangle;\quad T_2(\mathbf{p},\mathbf{Q}) = \langle\tilde{\Phi}^-(\mathbf{p})|e^{i\mathbf{Q}\cdot\mathbf{r_2}}|\Phi_0\rangle;$$

$$T_3(\mathbf{p},\mathbf{Q}) = \langle\tilde{\Phi}^-(\mathbf{p})|\Phi_0\rangle\langle\Phi_0|e^{i\mathbf{Q}\cdot\mathbf{r}}|\Phi_0\rangle. \tag{9}$$

The tilde in Eq. (9) means that the continuum wave function is not symmetric anymore. Since in the atomic units $k = \omega/c$ ($c = 137$), the momentum transfer is $Q = k_1\sqrt{1-2t\cos\theta+t^2}$, where θ is the scattering angle of the photon, i.e. the angle between the vectors $\mathbf{k_1}$ and $\mathbf{k_2}$. The variable

$$t = \left(1-\frac{I_p+E_e}{\omega_1}\right),$$

determines the energy of the final photon, since $\omega_2 = \omega_1 t$.

1.2. Physical mechanisms

The first term T_1 in sum (8) describes the process, where electron 1 (active) both absorbs and emits a photon, acquires a momentum transfer $\mathbf{Q}$ and leaves the atom. In the exponential, the momentum $\mathbf{p}$ is subtracted from the momentum $\mathbf{Q}$, and T_1 depends therefore on the momentum $\mathbf{q} = \mathbf{p} - \mathbf{Q}$. This momentum is, in fact, the momentum of the bound active electron in the atom initially being at rest, since $\mathbf{q} + \mathbf{K} = 0$. This is the direct process, which plays the crucial role in the reactions of scanning the momentum distributions in atoms, such as (e, 2e) [12,13]. The main contribution to the integral T_1 does not depend on the magnitude of the vectors $\mathbf{p}$ and $\mathbf{Q}$, but only on their difference. Of course, the active electron is described by a Coulomb wave, which somewhat distorts the effect of the plane wave description, but does not fundamentally change the effect of the term T_1 as a tool of dynamic spectroscopy.

The term T_2 in sum (8) describes a different physical process. Passive electron 2 absorbs a photon, but transfers its energy and momentum to electron 1 through the internal correlations. Electron 2 remains in the atom, whereas electron 1 flies out. Such a process is just impossible, if the electrons in the atom are not correlated in any way. Therefore, this matrix element rapidly decreases with increasing momenta Q and p, while its negative effect is leveled out.

The third term T_3 is artificial and goes down quickly, when Q and p increase.

Thus, the larger the values of Q and p are, the better Compton ionization works as a method of studying momentum distribution of the active electron in an atom. Let us estimate the energies of the initial photon and the scattering angles of the final

one, for which it is possible. For relatively small energy of the emitted electron $t \sim 1$ with a high accuracy. Let the photon energy be 10 keV. Then $\omega_1 = 10000/27.2 = 367.6$ a.u. and $k_1 = 2.68$. We require the condition $Q \sim p$ to be fulfilled. This is the so-called Bethe-ridge, where the ion recoil momentum $K = 0$, and the differential cross section of the process $(e, 2e)$ reaches its maximum. Then $E_e \sim k_1^2/2(1 - 2t\cos\theta + t^2)$ and $k_1^2/2 \approx 98$ eV. The momentum transfer reaches its maximum for backscattering, i.e. $Q_{max} \sim 2k_1$. Thus, $0 < E_e \lesssim 390$ eV, and larger energies of the emitted electrons are achieved, when photons are backscattered.

Hence it follows that the larger the cutoff angle θ_0 of the scattered photons is, beyond which we collect the statistics of coincidence events, the closer the total amplitude in (8) is to the term T_1, which gives information of spectroscopic value. Below we present some calculations and estimates.

2. Calculations and discussion

Despite the possibility of highly informative coincidence measurements, cross sections (6) are still rather small, and one has to measure various integral cross sections, from which it is also possible to extract useful information about the structure of an atomic target. However, in the present paper we are interested in the role of various terms in expression (8). To this end, we calculate the single differential cross section

$$SDCS_p = \frac{d\sigma}{dE_e} = 2\pi \int_0^{\pi} \sin\chi\, d\chi \int_0^{2\pi} d\phi \int_{\theta_0}^{\pi} \sin\theta\, d\theta \quad FDCS \tag{10}$$

in the electron energy range $0 < E_e < 150$ eV for four cutoff angles $\theta_0 = 0, 20^\circ, 30^\circ, 90^\circ$. The angle χ is the angle between the momentum of the emitted electron and the momentum of the incident photon $\mathbf{k_1}$ (axis z), the angle ϕ is the angle between the planes formed by vectors $(\mathbf{k_1}, \mathbf{k_2})$ and $(\mathbf{k_1}, \mathbf{p})$. To make the estimates, we use the simplest Hylleraas (Hy) model of the wave function of helium atom

$$\Phi_{Hy}(\mathbf{r_1}, \mathbf{r_2}) = \phi(r_1)\phi(r_2), \quad \phi(r) = \sqrt{\frac{Z^3}{\pi}} e^{-Zr}, \quad Z = 27/16.$$

In each of the four plots in Fig. 1, the contribution of only the T_1 term (solid curves) and the sum of all three terms in Eq. (8) are shown.

As it was expected, the dashed line approaches the solid line of T_1 with increasing electron energy and the growth of the momentum transfer. Of course, there must be a balance between achieving small contributions of the undesirable terms T_2 and T_3 and the accumulation of statistics. Fig. 1 shows that although the cross section seems to be small at $\theta_0 = 90^\circ$, it is not the case. It grows and reaches its maximum at the electron energy close to $E_e \sim Q^2/2$. For convenience of estimating the cross-section value, we can convert the atomic units to more common units: 1 a.u. $= 10^6$ barn/(eV $\cdot$ Sr ^{2}).

We see the same trend in Fig. 2, although here a helium ground state function with intensive radial and angular electron correlations is used [14,15], which we denote by CF:

$$\Phi_{CF}(\mathbf{r_1}, \mathbf{r_2}) = \sum_{j=1}^{10} D_j (e^{-a_j r_1 - b_j r_2} + e^{-a_j r_2 - b_j r_1}) e^{-\gamma_j r_{12}}.$$

This function provides the helium ground state energy $\varepsilon_0^{CF} = -2.90371$ a.u., which is practically very close to its experimental value $\varepsilon_0^{exp} = -2.903724$ a.u. In various previous calculations in other models, this function gave the best fit of experimental data, in particular, in paper [1]. A comparison of Figs. 1 and 2 confirms the known fact that the single differential cross sections are less sensitive to the correlation details of the helium ground state. The total cross section does not depend on such details at all.

In this connection, the following remarks should be made. The helium atom as an object for various kinds of theoretical research in the scattering theory is studied for a long time already, and there are innumerable test wave functions of this atom. However, in the case of other multi-electron atoms, the theory has not advanced far beyond the scope of the Hartree-Fock method, which has recently been joined by the density functional theory (DFT). For relevant calculations, the Clementi-Roetti [16] tables of trial wave functions of atoms up to $Z = 54$ and their ions are widely used. For this reason the simplest Hylleraas function used above for the estimates is not so simple against this background. We note that the wave function of the helium atom, taken from these tables, gives practically the same curves as those in Fig. 2.

Of course, for the purposes of studying the momentum distribution of the active electron in an atom, it is required that recoil momentum $\mathbf{q} = \mathbf{p} - \mathbf{Q}$ be of the order of a few atomic units (for quasielastic (e, 2e) reactions it is usually 2 - 3 a.u., after which, depending on the shell under study, distortions begin to appear). Therefore, the fact that for $\theta_0 = 90^\circ$ the term T_1 dominates in Fig. 2 at $E_e \sim 30$ eV does not mean that spectroscopic studies can be carried out at these energies. In all cases $p \sim Q$, which discriminates the types of electron detectors by their energy resolution power for use in the COLTRIMS device. It is useful to compare the CMS method with the widely known (e, 2e) EMS method in the kinematics of a quasi-elastic impact, which we now turn to.

2.1. Comparison with (e,2e) dynamical spectroscopy

Electron momentum spectroscopy in quasielastic impact kinematics [12,13] is one of the most powerful methods of studying the momentum distribution of an active electron in an atom. In the experiment, a fast projectile electron knocks out also a fast electron from the target, and both final electrons have approximately equal energies and the angles $\sim 45^\circ$ with respect to the bisector of the angle between them. For fast projectile electrons, the momentum transfer Q is rather large in this case. The laws of conservation of energy and momentum are similar to those in Eq. (1):

$$E_0 = E_1 + E_2 + I_p + E_{ion},$$

$$\mathbf{p_0} = \mathbf{p_1} + \mathbf{p_2} + \mathbf{K}.$$

In the experiments, by changing the energy or azimuthal angle of the projectile electron, experimenters achieve a signal from the required shell with a single ionization potential I_p, and then, slightly changing the angles of final electrons, they obtain the momentum profile of the wave function of the active electron initially present in this shell. The recoil momentum $\mathbf{q} = -\mathbf{p_0} + \mathbf{p_1} + \mathbf{p_2}$ is precisely its momentum in the target initially at rest, since $\mathbf{K} + \mathbf{q} = 0$.

In the plane-wave impulse approximation (PWIA), the triple differential cross section (3DCS) takes the form

$$\frac{d^3\sigma}{dE_2 d\Omega_e d\Omega_1} = 2\frac{p_1 p_2}{(2\pi)^3 p_0} (d\sigma)^{Mott} |T_1|^2. \tag{11}$$

$$T_1 = < \mathbf{p_1}, \mathbf{p_2}, \phi^{He^+} \left| e^{i\mathbf{Q}\cdot\mathbf{r_1}} \right| \mathbf{p_0}, \Phi_0 > = \int d^3 r_1\, e^{-i\mathbf{q}\cdot\mathbf{r_1}} \int d^3 r_2\, \varphi_0^{He^+}(\mathbf{r_2}) \Phi_0(\mathbf{r_1}, \mathbf{r_2}). \tag{12}$$

In (12) $\mathbf{Q} = \mathbf{p_0} - \mathbf{p_1}$, and the Mott cross section

$$d\sigma^{Mott} = \frac{4}{Q^4} \left(\frac{2\pi x}{\exp(2\pi x) - 1} \right) \left[1 + y^4 - y^2 \cos(2x \ln y) \right]$$

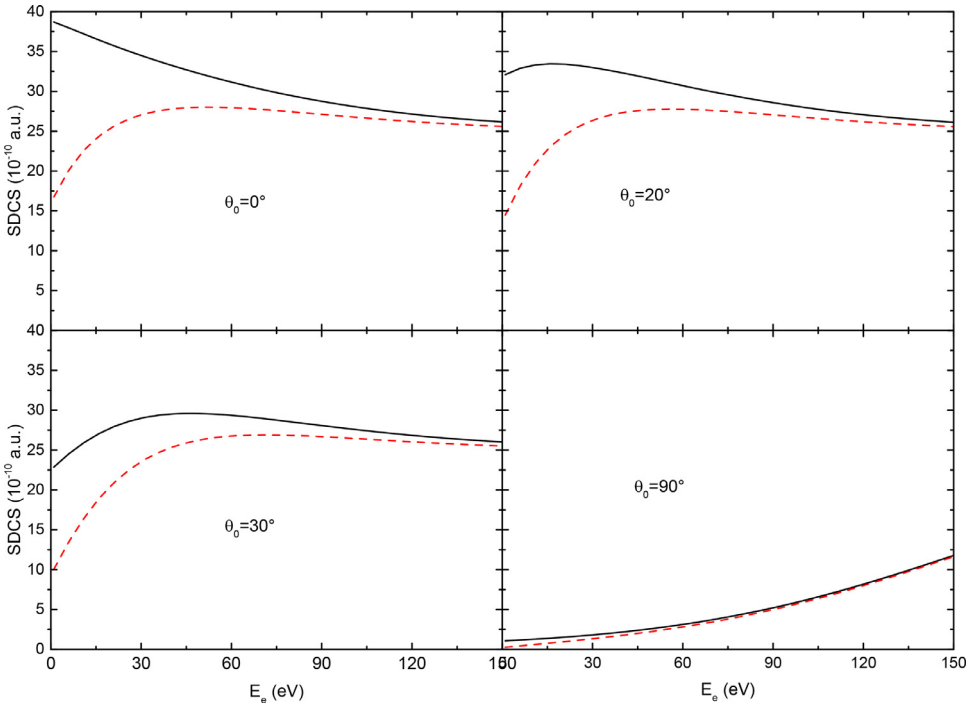

Fig. 1. SDCS as a function of the emitted electron energy E_e in the case of the Hy ground helium wave function. The photon energy is $\omega = 10$ keV. The cutoff angles θ_0 are shown in the figures. The solid (black) curve is the result of the calculation with only T_1, the dashed (red) curve is the sum of all terms in Eq. (8).

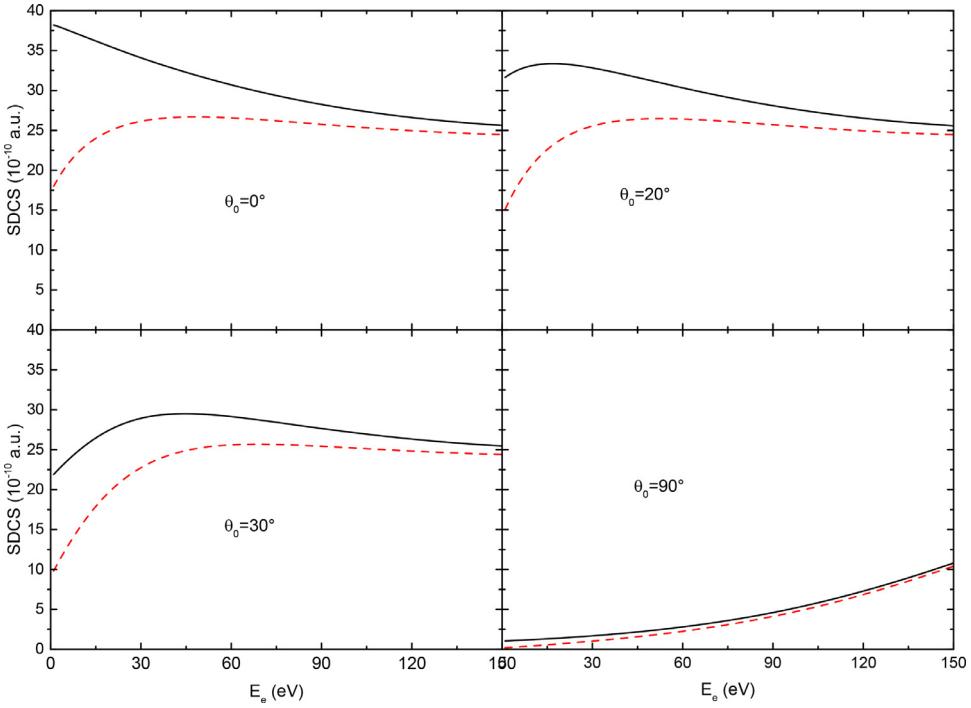

Fig. 2. The same as in Fig. 1, but for the CF ground helium wave function.

with $x = |\mathbf{p_1} - \mathbf{p_2}|^{-1}$, $y = |\mathbf{p_0} - \mathbf{p_1}|/|\mathbf{p_0} - \mathbf{p_2}|$. For the pure EMS kinematics $y = 1$.

Let us pay attention to the amplitude T_1 in Eq. (12). The diagram of the scattering process in the PWIA approximation, which gives rise to this amplitude, is schematically shown in Fig. 3. According to this diagram, it is precisely the Fourier transform of the one-particle wave function of the active electron contained in a certain shell of the atom, which determines the profile of its momentum distribution. This matrix element is similar to T_1 in Eq. (9) taking into account the final state wave function in the form of Eq. (7).

At this point, a comment on the applicability range of the plane wave approximation is needed. In Eq. (12), for simplicity of the physical picture, we have neglected the fact that both emitted electrons are in the field of the residual ion, and should be described by distorted (Coulomb) waves. Moreover, to describe the three-particle Coulomb continuum, the so-called 3C function is often used, which takes into account the interaction of the two electrons

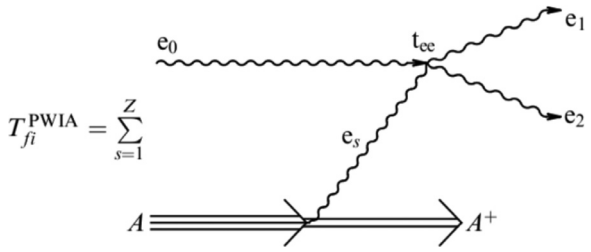

Fig. 3. The diagram of the process (e, 2e) in the plane-wave impulse approximation. The summation is carried out over all electrons in the target contained in the shell under study. For a helium atom, $Z = 2$.

and the ion and gives the correct three-particle Coulomb asymptotics [17].

The question of PWIA validity and its applicability range is actively discussed in the literature (see, for example, [19,20]). Numerous calculations show that PWIA successfully works for initial energies of at least 5 keV, and only when studying external shells. Otherwise, to achieve a coincidence of calculations with the experiment, one has to use the distorted-wave Born (impuls) approximation (DWBA, DWIA) [21], which destroys the attraction of the (e,2e) EMS reactions as a direct method of dynamic momentum spectroscopy. Thus, even for relatively large energies of the final electrons and large momentum transfers, the final wave function is not trivial.

Note that the matrix element T_1 in Eq. (9) is much simpler, because it includes only one Coulomb wave in the final state. Replacing it by a plane wave, we immediately obtain Eq. (12). Of course, there remains the problem of distortion of the electron plane wave by the atom field after the ionization, the distortion being especially strong for the inner shell electrons, which prevents the use of low energy electrons for the purpose of momentum spectroscopy.

Thus, the question arises, at what energy can we consider the Coulomb wave to be almost a plane wave and obtain a pure momentum profile of an active electron from Eq. 5? We immediately note that this issue has been discussed in the literature for many years, and there is still no clarity. This topic is partially covered in review [18]. To investigate the problem of the "transformation" of a Coulomb wave into a plane wave in this case, we note that the value of $q = |\mathbf{Q} - \mathbf{p}|$ must be limited, since the momentum of an active electron in an atom is expected to be small, and its large values lie at the distribution boundary. The minimum value $q = 0$ (the so-called Bethe-ridge, when the entire momentum transfer is given to the electron) is reached under the condition $\mathbf{Q} = \mathbf{p}$. If we increase the electron energy, we must accordingly change the scattering angle of the photon also increasing it. Fortunately, in contrast to the (e, 2e) reaction, where the momentum transfer is in the denominator of the cross section as Q^4, because the interaction is mediated by a virtual photon (Coulomb potential), there is no such thing here, since the interaction occurs with a real photon, and we can increase both Q and E_e. However, such options are restricted by the capabilities of experimental detector devices.

The boundary value of momentum transfer, which is achieved in this problem at $\theta = 180^\circ$, is equal to $Q^{max} = 2k_1 = 5.36$ a.u., which corresponds to the maximal electron energy $E_e^{max} = 390$ eV. We will again choose the simplest model Hy (helium ground state)+ CW (Coulomb wave of emitted electron) for estimations. In this case, from Eq. (9) we have $Z = 27/16$:

$$T_1(\mathbf{p}, \mathbf{Q}) = \langle \tilde{\Phi}^-(\mathbf{p}) | e^{i\mathbf{Q}\cdot\mathbf{r}_1} | \Phi_0 \rangle = -\sqrt{\frac{8}{\pi}} \left(\frac{2Z}{Z+2} \right)^3 \frac{\partial}{\partial Z} I(\mathbf{Q}, \mathbf{p}, Z). \tag{13}$$

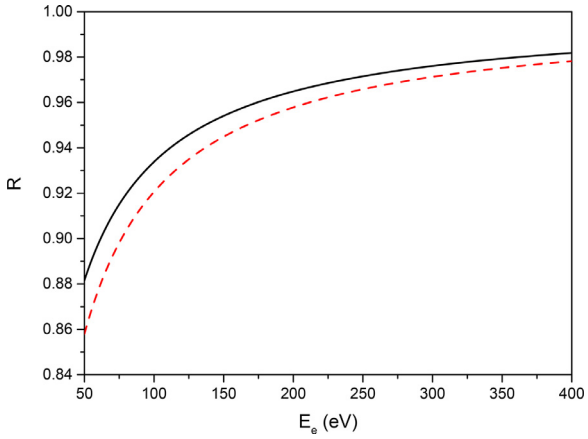

Fig. 4. Ratio R Eq. (15), $q = 0$. Black (solid) curve: Hy wave function, red (dashed) curve: CF wave functions

In (13)

$$I(\mathbf{Q}, \mathbf{p}, Z) = 4\pi R(\xi) \frac{[(Z - ip)^2 + Q^2]^{i\xi}}{[(\mathbf{Q} - \mathbf{p})^2 + Z^2]^{1+i\xi}}, \tag{14}$$

and

$$R(\xi) = \exp(-\pi\xi/2)\ \Gamma(1 + i\xi),\ \ \xi = -1/p.$$

If we put $\xi = 0$ in Eq. (14), we get the plane wave approximation

$$I^{PW}(\mathbf{Q}, \mathbf{p}, Z) = \frac{4\pi}{(\mathbf{Q} - \mathbf{p})^2 + Z^2}. \tag{14.1}$$

We calculate the ratio

$$R = \left| T_1 / T_1^{PW} \right|^2, \tag{15}$$

which is shown in Fig. 4. It can be seen from the figure that for $E_e = 50$ eV, which is considered to be rather large, the difference between the plane and Coulomb wave effects is 12–14% both for simple Hy and complex CF ground helium wave functions. At $E_e =$ 390 eV the difference goes down to 2%. The shapes of both curves are practically the same, and here again the question rests on the capabilities of high-energy electron detectors.

Now we estimate the ratio of the FDCS (5) and 3DCS (11) supposing that the momentum profile is defined in both cases by Eq. (12). We assume for (e,2e) equal final (large) electron energies and equal angles about 45°. In the atomic units, this ratio is equal to

$$\frac{FDCS}{3DCS} \approx \frac{\alpha^4}{\sqrt{2}} E_e^2. \tag{16}$$

Of course, this ratio is proportional to the small factor α^4, but increases with the growth of the energy of the emitted electron. For $E_e \sim 400$ eV, the value $E_e^2/\sqrt{2} \sim 150 \sim c$ a.u. However, we have to note that the distortions of the final electron state at this energy are still rather large for the PWIA model to be used.

2.2. Possible experiment setting to get the momentum profile of the active electron from CMS

Let us discuss the setup of a possible CMS experiment. Recall that in this experiment, the electron and ion momenta are measured in coincidence, and the energy and momentum of the final photon and, accordingly, the momentum transfer are calculated from the conservation laws. The most difficult problem of such experiments is the determination of the shell, from which the ionization occurs. Helium has only one shell, and there is no such problem here. However, experiments with the reaction (e,2e) in the EMS kinematics allow one to resolve, for example, 2s and 2p

shells in the neon atom. What is the situation here? We would like to put forward the following way. We write down the momentum transfer in the case of backward scattering $\theta = 180^\circ$. In this case, $Q = k_1(1+t)$. Next, we recall that the momentum transfer is expressed in terms of the experimentally measured momenta as $Q = |\mathbf{p}+\mathbf{K}|$. Let us consider the case, where the final photon scatters back and select the coincidence events, where the electron is emitted strictly forward, and the ion is recoiled strictly backward. Then we get the formula:

$$I_p = c[(2k_1 - p) + K] - \frac{p^2}{2} = const. \quad (17)$$

In principle, this relation is restricted by the inequality $I_p + E_e \leq \omega_1$. According to our choice of large electron momenta and relatively small ion momenta $K = q$, we consider the momenta $p \sim 2k_1$. In this paper, for our choice $\omega_1 = 10$ keV the electron energy is $E_e \lesssim 390$ eV. In order for ratio (16) to be positive, we need $(2k_1 - p) + K > 0.1$, which is quite reasonable.

However, this ideal picture cannot be actually realized with the COLTRIMS setup, since, with the increasing detectable electron energies, the momentum resolution for the ion generally decreases. We will discuss this point in more detail below.

Let us consider now, for simplicity, the plane wave instead of the Coulomb wave in the term T_1. In this case, this term in (9) will depend only on the ion momentum $K = q$. By measuring K, for example, in a narrow backscattering cone, we will be sure, even without measuring the electron momentum for coincidence, that these momenta are large. Thus, we will receive directly the momentum distribution of the active electron in the atom. However, without knowing the shell, from which the ionization occurred, we get the average distribution over all shells in the atom. The only exception among the many-electron atoms is the helium atom [22].

Thus, for future experiments the technically most challenging problem is to determine the final state of the ion produced by Compton scattering, i.e. to determine the shell from which the electron was ejected. This is problematic since a) the initial photon energy is not very well defined, because today the high flux needed to compensate for the small Compton cross section prohibits narrow monochromatizating of the incoming photons, and b) the electron energy resolution of a COLTRIMS spectrometer for high-energy electrons is insufficient for resolving valence subshells, and c) for heavier atoms and molecules the momentum resolution for the ion detection degrades. These problems can be overcome by adding a large area pixel detector for detecting the scattered photons such as DEPFET sensors [23]. Such detectors can be read out at MHz rates and can detect single photons. The polar and azimuthal scattering angle of the photons can be detected in coincidence with the polar and azimuthal angle of the ejected electron and the recoil ion. However, for the latter two the magnitude of the momentum is detected only with insufficient resolution. Such a realistic photon-electron-ion coincidence would have large enough solid angle and it would determine a total of 6 linearly independent quantities. This is sufficient to fully characterize Compton scattering including the energy of the final ionic state. In the final state there are 9 momentum components (scattered photon, electron, ion) and the excitation energy of the ion to be determined. From these 10 quantities only 6 are linearly independent since there are a total of 3 conservation laws for the three momentum components and additionally energy conservation.

3. Conclusion

In the present paper we have shown that the process of single Compton ionization of an atomic target has a good potential for being used as a tool for studies of the momentum distribution of an active electron in the helium atom. This becomes possible at relatively high energies of the emitted electron and, accordingly, at large momentum transfers Q, where the contributions of the undesirable terms T_2 and T_3 are reduced. Wherein the quantity $q = |\mathbf{Q} - \mathbf{p}| = K$ just determines the momentum of the active electron inside the target before its interaction with the photon, and this momentum should be small. Changing the angles and magnitudes of the vectors $\mathbf{Q}$ and $\mathbf{p}$, one can vary q in the required range.

With the current state of the art, the measurement of very small cross sections of Compton ionization is experimentally feasible, and therefore it could compete with other known methods of atomic spectroscopy, in particular, $(e, 2e)$ in the EMS kinematics. In this case, Compton ionization has a number of advantages from the point of view of theoretical interpretations. First, as the photon energy increases (remaining within the non-relativistic description of the scattering process), the range of electron energies and momentum transfers changes significantly without changing the value of the cross section in Eq. (5), if the momentum q remains small. Second, we can achieve a decrease in the influence of the undesirable terms T1 and T2 without changing the contribution of the T_1 term. Third, the final state is represented by only one electron, not two, which significantly reduces the choice of models for the final state, and therefore increases the reliability of determining the momentum distribution of the active electron in the target. Finally, fourth, the dominance of FBA (A^2) increases with increasing photon energy in comparison with SBA. We have not considered this issue in detail here due to space savings, but this is the case.

However, the COLTRIMS in its present day realization does not allow to determine the atomic shells, from which the ionization occurs, and, for this reason, it can be consistently applied to a limited number of many-electron targets (for example, helium atom, see also [24]). This significantly reduces the advantages of CMS as a method of dynamic spectroscopy in comparison with EMS. Although other applications of Compton single ionization are possible to processes with large electron momenta and small ion momenta for studying the ionization of light atoms, where the resolution of the electron shells is not necessary. A full realization of the CMS can be achieved in the future with new detectors, such as DEPFET sensors.

Declaration of Competing Interest

The authors declare that they have no known competing financial interests or personal relationships that could have appeared to influence the work reported in this paper.

CRediT authorship contribution statement

O. Chuluunbaatar: Software, Visualization. **S. Houamer:** Software, Visualization. **Yu. V. Popov:** Conceptualization, Writing – original draft, Supervision. **I.P. Volobuev:** Conceptualization, Writing – original draft, Writing – review & editing. **M. Kircher:** Writing – review & editing. **R. Dörner:** Conceptualization, Writing – review & editing.

Acknowledgements

The calculations were performed on the basis of a heterogeneous computing platform HybriLIT on supercomputer “Govorun” (LIT, JINR). The work was partially supported by the Hulubei-Meshcheryakov JINR programs, grant of RFBR and MECSS No. 20-51-4400, grant of Ministry of Science and Higher Education of the Russian Federation No 075-10-2020-117, grant of Foundation of Science and Technology of Mongolia SST 18/2018, grant of the RFBR No. 19-02-00014a. S.H. thanks the DGRSDT-Algeria Founda-

tion for support. R.D. and M.K. acknowledge funding by Deutsche Forschungsgemeinschaft (DFG).

Supplementary material

Supplementary material associated with this article can be found, in the online version, at doi:10.1016/j.jqsrt.2021.107820.

References

[1] Kircher M, et al. Kinematically complete experimental study of Compton scattering at helium atoms near the threshold. Nat Phys 2020;16:756–60. doi:10.1038/s41567-020-0880-2.
[2] Kramers HA, Heisenberg W. über die streuung von strahlung durch atome. Z Physik 1925;31:681–708.
[3] Waller I, Hartree DR. On the intensity of total scattering of X-rays. Proc Roy Soc(London) 1929;A 124:119–42.
[4] Compton AH. A quantum theory of the scattering of X-rays by light elements. Phys Rev 1923;21:483–502. doi:10.1103/PhysRev.21.483.
[5] Debye P. Zerstreuung von röntgenstrahlen und quantentheorie. Physikalische Zeitschrift 1923;24:161–6.
[6] DuMond JWM. Compton modified line structure and its relation to the electron theory of solid bodies. Phys Rev 1929;33:643–58. doi:10.1103/PhysRev.33.643.
[7] Bothe W, Geiger H. über das wesen des comptoneffekts; ein experimenteller beitrag zur theorie der strahlung. Z Physik 1925;32:639–63.
[8] Ullrich J. Recoil-ion and electron momentum spectroscopy: reaction-microscopes. Rep Prog Phys 2003;66:1463–545. doi:10.1088/0034-4885/66/9/203.
[9] I Akhiezer A, Berestetskii VB. Quantum electrodynamics. John Wiley and Sons; 1965.
[10] Bergström JPM, Suri N, Pisk K, Pratt RH. Compton scattering of photons from bound electrons: full relativistic independent-particle-approximation calculations. Phys Rev A 1993;48:1134–62. doi:10.1103/PhysRevA.48.1134.
[11] Houamer S, Chuluunbaatar O, Volobuev IP, Popov YV. Compton ionization of hydrogen atom near threshold by photons in the energy range of a few kev: nonrelativistic approach. Eur Phys J D 2020;74:81–9. doi:10.1140/epjd/e2020-100572-1.
[12] Weigold E, McCarthy IE. Electron momentum spectroscopy. NY: Kluwer; 1999.
[13] Neudatchin VG, Popov YV, Smirnov YF. Electron momentum spectroscopy of atoms, molecules and thin films. Physics– Uspekhi 1999;42:1017–44. doi:10.1070/PU1999v042n10ABEH000492.
[14] Chuluunbaatar O, Puzynin IV, Vinitsky PS, Popov YV, Kouzakov KA, Cappello CD. Role of the cusp conditions in electron-helium double ionization. Phys Rev A 2006;74:014703. doi:10.1103/PhysRevA.74.014703.
[15] Chuluunbaatar O, Puzynin IV, Vinitsky PS. Uncoupled correlated calculations of helium isoelectronic bound states. J Phys B: At Mol Opt Phys 2001;34:L425–32. doi:10.1088/0953-4075/34/14/101.
[16] Clementi E, Roetti C. Roothaan - Hartree - Fock atomic wave functions. At D Nucl Data Tables 1974;14:177–478. doi:10.1016/S0092-640X(74)80016-1.
[17] Brauner M, Briggs JS, Klar H. Triply-differential cross sections for ionisation of hydrogen atoms by electrons and positrons. J Phys B 1989;22:2265. doi:10.1088/0953-4075/22/14/010.
[18] Shablov VL, Vinitsky PS, Popov YV, Chuluunbaatar O, Kouzakov KA. Born series in the theory of electron impact ionization of an atom. Phys Part Nucl 2010;41:335–57. doi:10.1134/S1063779610020048.
[19] Miyake Y, Takahashi M, Watanabe N, Khajuria Y, Udagawa Y, Ya S, Mukoyama T. Examination of (e,2e) scattering models by comparison of momentum profiles of noble gases between experiment and theory. Phys Chem Chem Phys 2006;8:3022–8. doi:10.1039/b603117j.
[20] Watanabe N, Takahashi M, Udagawa Y, Kouzakov KA, Popov YV. Two-step mechanisms in ionization-excitation of he studied by binary (e,2e) experiments and second-born-approximation calculations. Phys Rev A 2007;75:052701. doi:10.1103/PhysRevA.75.052701.
[21] McCarthy IE. Distorted-wave born and impulse approximations for electron-atom ionisation. Aust J Phys 1995;48:1–17. doi:10.1071/PH950001.
[22] Kaliman Z, Pisk K. Compton cross-section calculations in terms of recoil-ion momentum observables. Radiat Phys Chem 2004;71:633–5. doi:10.1016/j.radphyschem.2004.04.035.
[23] Richter RH. Design and technology of DEPFET pixel sensors for linear collider applications. Nucl Instrum Methods Phys Res A 2003;511:250–6. doi:10.1016/S0168-9002(03)01802-3.
[24] Kircher M. Photon-momentum-induced molecular dynamics in photoionization of n_2 at $h\nu = 40$ kev. Phys Rev Lett 2019;123:193001. doi:10.1103/PhysRevLett.123.193001.